On the Dynamics of Turing Pattern Formation in 1D CNN's

By
Teodorescu Tiberiu and Liviu Goras

Abstract

The aim of this communication is to point out several aspects related to the initial conditions influence on Turing pattern formation in simple 1D CNN's based on the reduced Chua's circuit. Using spectral analysis the correlation between initial conditions and final pattern spectra are investigated. It is also shown that the results of the simulations may drastically depend on the specific ways of number representations in computers.

Introduction

Turing patterns formation in CNN's is a rather recent area of research in nonlinear circuit theory […]. Even the analysis of pattern formation is a genuine nonlinear problem, it has been shown that significant insights may be obtained using linear theory, especially the technique of spatial mode separation […], which applies mainly in the case of piece-wise linear nonlinearities. In such cases, the shape and the position dispersion curve together with the weights of the spectral components in the initial conditions determine the evolution towards the final pattern.

Many simulations have been done using random initial conditions generated by the C-programming medium supposed to have a homogeneous spectral composition (equal weights of the spectral lines), an assumption which is often far from being true. This matter is considered in certain detail in this communication.

Usually, the notion of *pattern* refers to stable equilibrium points. However, we are going to show that, for special initial conditions, the patterns obtained through computer simulation may correspond to unstable equilibrium points as well. In such situations, the noise related to the internal representation of numbers in the computer (truncation) may play a significant role, qualitatively different patterns being able to appear depending on the way the initial conditions are introduced.

Before proceeding, we point out the fact that the notion of *mode* will be used with the significance of either temporal or spatial. We stress the fact that, for piece-wise nonlinearities, as soon as the first cell enters the nonlinear portion of its characteristic, there are no more relations between the corresponding temporal eigenvalues and the spatial modes.

Spectral mapping through CNN dynamic evolution

All simulations have been made using the cell based on Chua's reduced circuit represented in **Fig. 1:**

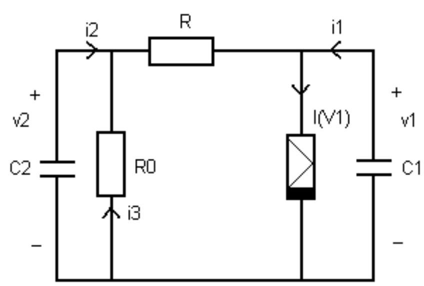

Fig. 1 Chua's reduced circuit

The parameters of the cell are the following (we will keep the original notations from [...]): Gamma=50 (3-cell zero-flux CNN) Gamma=85 (4-cell ring CNN), D_u=1, D_v=75, f_v=-1, g_u=0.1, g_v=-0.2, m_1=m_2=-1, m_0=0.1. First, we have investigated the behavior of a 1D 3-cell zero-flux CNN and 4-cell ring CNN for two sets of random initial conditions generated with the same mechanism. We show that even in this very simple case two different patterns may evolve, depending on the spectral composition of the initial conditions. For the 3-cell case the temporal eigenvalues have been calculated for the situation when all cells are in the central part of the nonlinear characteristic, two eigenvalues being in the right-side complex plane (The corresponding real parts are 1,0963 and 0.9404).

When the center cell is in the nonlinear part of the characteristic, there still exist an eigenvalue with positive real part (0.9404), which happens to have the same value with the previous case. The results for the 3-cell CNN are shown in **Fig. 2a**, **b**, **c**, **d** and **Fig. 3a**, **b**, **c**, **d** which represent respectively the spectrum of the initial conditions, the spectrum just before entering the nonlinear region, the spectrum of the final pattern and the pattern for two sets of initial conditions obtained using the subroutine *randomize()*.

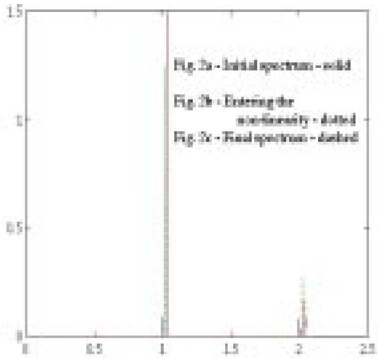

It is obvious that the spectra of the two initial conditions are different leading to two different patterns.
For the 4-cell CNN case the real parts of the temporal eigenvalues within the right hand plane computed for the situation when all cells are in the central part of the nonlinear characteristic are 2.2307 and 2.2368.

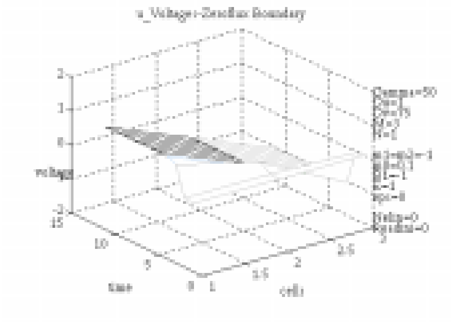

Fig. 2d Final pattern

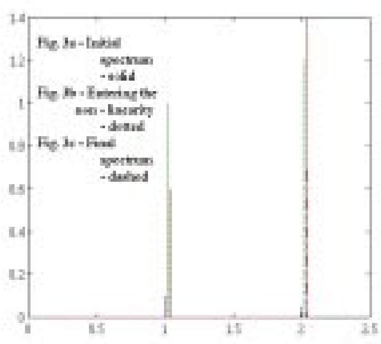

When the cells 2 and 4 are in the nonlinear part of the characteristic, there still exists an eigenvalue with positive real part (2.2307), which happens to have the same value as in the previous case.

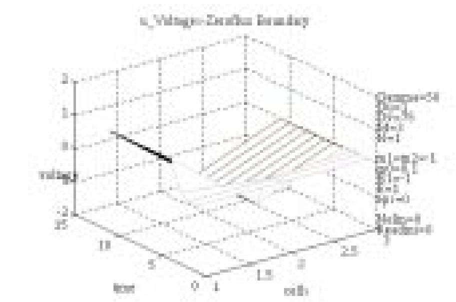

Fig. 3d Final pattern

The results for the 4-cell CNN are shown in **Fig. 4a, b, c, d** and **Fig.5 a, b, c, d** which represent respectively the spectrum of the initial conditions, the spectrum just before entering the nonlinear region and the spectrum of the final pattern for two sets of initial conditions obtained using the same subroutine *randomize ()*.

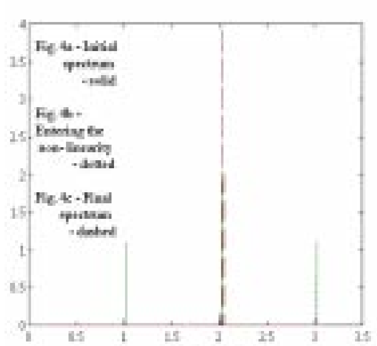

It is obvious that the spectra of the two initial conditions are different leading to two different patterns.
In the next simulations the initial conditions which have been used were a combination between deterministic and randomly generated ones. Let us consider the 3-cell zero-

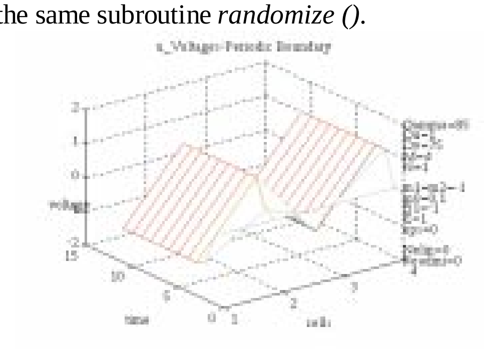

Fig. 4d Final pattern

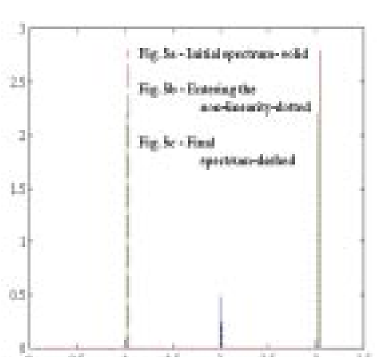

flux CNN case. There are two temporal modes inside the domain of instability in the dispersion curve [...]. We will simulate the network with initial conditions which contains one of the two modes and in adding a level of noise generated by C. We want to the network in others than the corresponding patterns of initial modes at an insignificant level of noise.

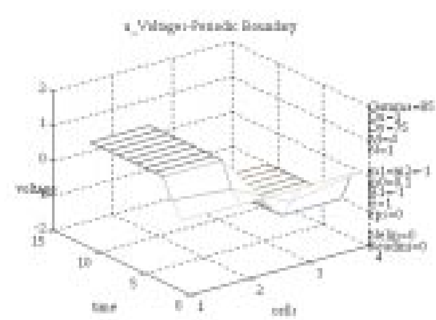

Fig. 5d Final pattern

For the first time we'll seed the network with mode 1 added to a level of noise by 100% and then will initialize the network with mode 2 added to a level of noise by 200%. The results are similar with **Fig. 2d** and respectively **Fig. 3d**.

In the first case we see that one obtain a pattern whose spectrum corresponds to the initial spectrum increased. The second pattern is the one that has a component from the initial conditions added to other component given by mode 2 being present because of the spectrum of noise.

We are studying now the mode 2 added to an insignificant level of noise: 1/1000*mode 1. The results are given in **Fig. 6a** and **b**.

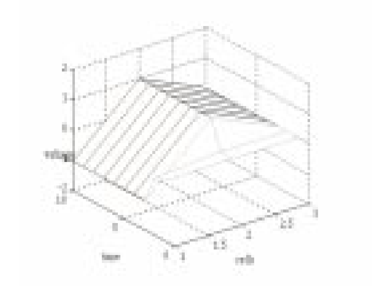

Fig. 6a Mode 2 + 1/1000 noise – final pattern

We notice that the final pattern's spectrum contains "mode 2" and "mode 1".

The conclusion of these two experiments is that different modes and their corresponding patterns have different levels of robustness. We will see that spectral mapping is related to the nature of the equilibrium points (stable or unstable) and to their corresponding patterns.

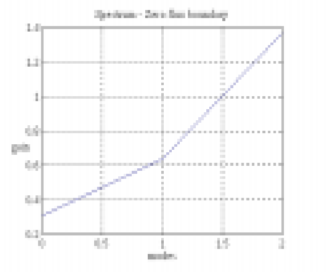

Fig. 6b It's corresponding final spectrum

Stable and unstable patterns

We will study the equilibrium points in the case of the zero-flux boundaries. Other cases are similar to that case. Equilibrium points can be stable or unstable. For the network with the topology presented in [...] we will define the equilibrium stable points as that points from the state space for which there are only eigenvalues with negative real part. The other points will be that points which have at least one eigenvalue with positive real part. The stable equilibrium points will be that points in which the network's state will remain unchanged for an indefinite time and the unstable points will be that points from which the network will leave at a small noise.

We can give now one stop condition for an algorithm that calculate the evolution of the network: It only stops in states in which the difference between a state and the other is unnoticeable and, added to this condition, the network should have reached a state (a combination of segments in the piece-wise linear characteristics) which has no positive real parts for its eigenvalues. If the network stop in an point of equilibrium in which all cells reached the nonlinearity, then the algorithm stops too.

We will consider the 3-cell case. The state equations have the following shape:

$$\dot{\begin{bmatrix} u_1 \\ u_2 \\ u_3 \\ v_1 \\ v_2 \\ v_3 \end{bmatrix}} = \begin{bmatrix} \gamma f_u & D_u & 0 & \gamma f_v & 0 & 0 \\ D_u & \gamma f_u - 2D_u & D_u & 0 & \gamma f_v & 0 \\ 0 & D_u & \gamma f_u - D_u & 0 & 0 & \gamma f_v \\ \gamma g_u & 0 & 0 & \gamma g_v - D_v & D_v & 0 \\ 0 & \gamma g_u & 0 & D_v & \gamma g_v - 2D_v & D_v \\ 0 & 0 & \gamma g_u & 0 & D_v & \gamma g_v - D_v \end{bmatrix} \begin{bmatrix} u_1 \\ u_2 \\ u_3 \\ v_1 \\ v_2 \\ v_3 \end{bmatrix}$$

In this system of equations we will name the matrix A. We will initialize the network with mode 2. This will develop up to the pattern shown in **Fig. 7 a**.

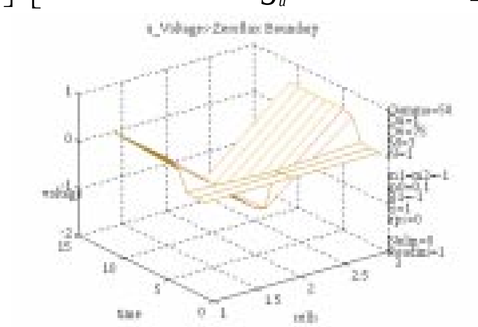

Fig. 7a Pattern from 'clean' 2-mode

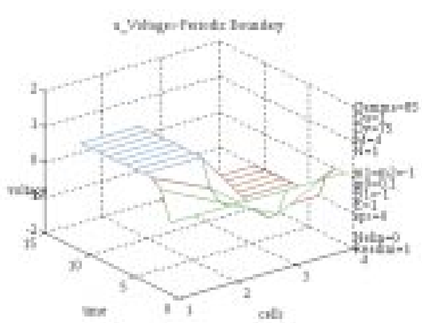

Fig. 7b Entering the nonlinearity and final pattern (init with mode 1)

Related to the voltages of the u-nodes, in this case, the cells 1 and 3 will be placed on the region containing the origin of the nonlinear resistor, and the cell 2 will be placed on the left region of the nonlinear characteristic. This leads to the modification of the characteristic polynom, and consequently to the eigenvalues' changing. The only eigenvalue with a positive real part in this situation is 1.0963.

It is noticed that the above mode remains the only one in the band. This means that, at the slightest noise, this equilibrium point being, by definition, unstable, the network ‘ will leave’ it. Therefore, it is achieved the pattern from **Fig. 3d**, whose spectral components are shown in **Fig. 3c**. It is noticed that an unchanged eigenvalue exists between the first regions’ combination and the second.

$$\begin{bmatrix} \dot{u}_1 \\ \dot{u}_2 \\ \dot{u}_3 \\ \dot{u}_4 \\ \dot{v}_1 \\ \dot{v}_2 \\ \dot{v}_3 \\ \dot{v}_4 \end{bmatrix} = \begin{bmatrix} \gamma f_{u1}-2D_u & D_u & 0 & D_u & \gamma f_v & 0 & 0 & 0 \\ D_u & \gamma f_{u2}-2D_u & D_u & 0 & 0 & \gamma f_v & 0 & 0 \\ 0 & Du & \gamma f_{u3}-2D_u & Du & 0 & 0 & \gamma f_v & 0 \\ D_u & 0 & D_u & \gamma f_{u4}-2D_u & 0 & 0 & 0 & \gamma f_v \\ \gamma g_u & 0 & 0 & 0 & \gamma g_v-2D_v & Dv & 0 & D_v \\ 0 & \gamma g_u & 0 & 0 & D_v & \gamma g_v-2D_v & D_v & 0 \\ 0 & 0 & \gamma g_u & 0 & 0 & D_v & \gamma g_v-2D_v & D_v \\ 0 & 0 & 0 & \gamma g_u & D_v & 0 & D_v & \gamma g_v-2D_v \end{bmatrix} \begin{bmatrix} u_1 \\ u_2 \\ u_3 \\ u_4 \\ v_1 \\ v_2 \\ v_3 \\ v_4 \end{bmatrix}$$

A similar situation was obtained for the case 4-cell ring CNN. Matrix A is also given below. If we initialize the network with mode 1, this will develop up to the pattern shown in **Fig. 7 b**. Related to the voltages of the u-nodes, in this case the cells 2 and 4 will be placed in the left region of the nonlinear resistor and respectively the cells 1 and 3 will be placed on the region containing the origin of the nonlinear resistor. This leads to the modification of the characteristic polynom, and consequently to the eigenvalues’ changing. The only eigenvalue with a positive real part in this situation is 2.2307. Let us notice an important thing: this eigenvalue is the same that mode 1 had at the beginning of the simulation (when all cells had the same near – origin position on the nonlinear characteristic). But, because this mode was seeded at the beginning, and the nonlinearly was reached for all cells the network will not evolve from this point. In the case when we seed the network with mode 2, this mode is developing to a state that has not an eigenvalues with positive real part.

Considerations related to the numerical method and concluding remarks

Taking into account the 3 cells- 1D situation it is brought up to date that for the simulation using as initial conditions mode 2 plus noise, mode 2 was distorted by an insignificant noise level. As it was presented above, at the end of the mode 2 growth, the network emerges in an unstable point of equilibrium, this being already demonstrated. We can ascertain that in the absence of the other circumstances’ influence, the existence of the eigenvalue with positive real part led to the fact that at any level of noise, the system should leave this point of equilibrium. The robustness of a mode related to the noise is linked in the case of simulation through the spectral composition of the noise, through the difference between the real part of the two concurrent modes. It is very important that the robustness depends on the existence of the unstable points of equilibrium and on the accuracy of the internal representation on the computer. In a real case (physical reality) all the circumstances are preserved except the spectral composition of the noise (one assumes that white noise does exist in nature) and internal representation.

The numerical method was EULER algorithm with a constant step. When are setting up mode 2 with the expressions given in References, because of the internal representation a mode 1 component occurred, developing apparently unjustified. But when mode 2 has been set up manually (with precise values) this mode 1 component has not occurred; it was only the 2 ‘clean’ mode that occurred in **Fig.7a**. This is very well connected with the simulations done for setting up the network with mode 2 plus noise. In this case ‘ the noise generator’ was the computer itself, like in the case presented below; we used an scheme done in Simulink and we obtained the next evolution for the cells (Ox axes is time and Oy is voltage; The domain for time is 0 ÷ 50 units and for the voltage is –1 ÷1 volts for cells 1 and 3 and –1.5 ÷ 1.5 volts for the center cell):

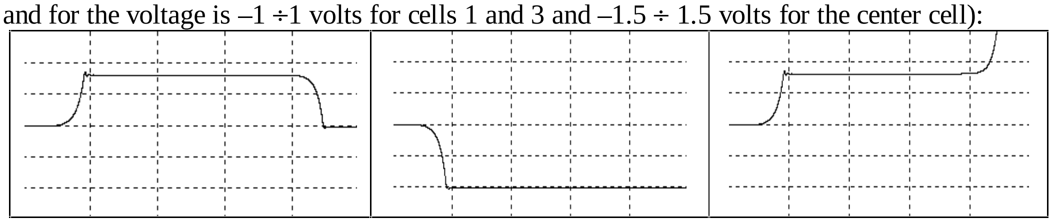

Fig. 8 The evolution of the voltages for the cells (from left to right cell 1, 2 and 3)

We see from this graphical presentation that the voltages for cells 1 and 3 remain a time at 0.5 volts and then they leave this unstable state and reach the nonlinearity.

References

[1] L. Goraş, L.O. Chua, and D. M. W. Leenaerts - “Turing Patterns in CNN’s - Part I: Once Over Lightly”, article published in Circuits and Systems - A Publication of the IEEE Circuits and Systems Society, October 1995, volume 42, number 10, pp. 602 - 611

[2] L. Goraş and L.O. Chua - “Turing Patterns in CNN’s - Part II: Equations and Behaviors”, article published in Circuits and Systems - A Publication of the IEEE Circuits and Systems Society, October 1995, volume 42, number 10, pp. 612 - 626
[3] L. Goraş, L.O. Chua, and L. Pivka- - “Turing Patterns in CNN’s - Part III: Computer Simulation Results”, article published in Circuits and Systems - A Publication of the IEEE Circuits and Systems Society, October 1995, volume 42, number 10, pp. 627 - 637
[4] A. M. Turing, - “The chemical basis of morphogenesis”, Phil. Trans. Roy. Soc. Lond. B 237, pp.37 - 72, 1952